Aeolian Research 35 (2018) 29–38

Contents lists available at ScienceDirect

Aeolian Research

journal homepage: www.elsevier.com/locate/aeolia

A multi-proxy late Holocene climate record from aeolian deposits of the Horqin sandy land, northeast China and its societal implications

Shuang Zhao[a,*], Dunsheng Xia[b], Heling Jin[c], Jia Jia[b], Bing Liu[c]

[a] College of Geography and Tourism, Qufu Normal University, Rizhao 276826, China
[b] Key Laboratory of Western China's Environmental Systems (Ministry of Education), College of Earth and Environmental Sciences, Lanzhou University, Lanzhou 730000, China
[c] Key Laboratory of Desert and Desertification, Northwest Institute of Eco-Environment and Resources, Chinese Academy of Sciences, Lanzhou 730000, China

ARTICLE INFO

Keywords:
Climate change
Late Holocene
Aeolian deposit
Horqin sandy land

ABSTRACT

Late Holocene climate change is an important issue in global change research, because of its close relationship with human societal development. The Horqin sandy land is an important area for early dryland agriculture development. However, the role that climatic factors, especially temperature and precipitation, played in regional agriculture development is still unclear. This paper presents a high-resolution multi-proxy palaeomoisture record spanning 4300–1000 cal. yr BP derived from sequential aeolian sediments of the Liuhutun section on the northeastern frontier of the Horqin sandy land, northeast China. The 2.96 m section, with a chronology based on seven radiocarbon dates, was analyzed for sediment grain-size, $CaCO_3$ content, organic matter content and environmental magnetic parameters. The results indicate that 4300–3800 cal. yr BP was a humid period with a drying trend; that 3800–1700 cal. yr BP was generally dry; and that 1700–1000 cal. yr BP was sub-humid. It is clear that the regional climate was responsive to East Asian monsoonal circulation driven by variations in Northern Hemisphere summer insolation. We further investigate the relationship between climate change and regional agriculture development by comparing moisture records with regional temperature and subsistence strategy changes inferred from previous studies. The results suggest that high temperature and moderate precipitation may have facilitated agricultural development during the Lower Xiajiadian period (ca. 4000–3400 yr BP). Owing to the drought-tolerant and thermophilic phenological properties of millets, which are major crops of northeast China, temperature may have played a more important role in regional agriculture than precipitation.

1. Introduction

Because of rapid global warming at present, past climate change and its societal effects have received extensive concern (Hinsch, 1988; Wang et al., 2010; Fang et al., 2015). The late Holocene is the key period of human societal development and the study of climate change and its effects during that time may provide a valuable perspective on possible responses of modern societies to future climate change (deMenocal, 2001).

Aeolian deposits in the deserts and sandy lands are sensitive carriers of climate change information. Aeolian sand layers in the strata represent dune mobilization and dry climate, while palaeosol layers indicate dune stabilization and wet climate (Lu et al., 2005; Li and Sun, 2006; Zhou et al., 2008; Li et al., 2014). Chronostratigraphic studies of the aeolian deposits in the Horqin sandy land demonstrated that mobile sand dunes were built up during the Last Glacial Maximum (LGM), that dunes were stabilized and chernozem soils developed during the mid-Holocene, and that partial re-mobilization occurred since 3–2 kyr BP (Zhao et al., 2007; Yang et al., 2010, 2012; Yi et al., 2013). Based on time series of various proxies (e.g. pollen, grain-size and chemical elements) of aeolian sediments, researchers tried to reconstruct Holocene climatic history of the Horqin sandy land (Li et al., 2006; Liu et al., 2011; Yang et al., 2012; Mu et al., 2016), but high-resolution climate records are still scarce in this area.

The Horqin sandy land, situated on the West Liao River Plain, and more specifically, in the basin of the West Liao River, northeast China, is one of the 'cradles' of ancient Chinese civilization. Archaeological and archaeobotanical data demonstrate that a series of ancient cultures occupied this region since the early Holocene (Yang, 1994; Shelach, 1999; Linduff et al., 2002–2004), and that dryland agriculture began in this region from as early as 8–7.5 kyr BP (Zhao, 2011; Liu et al., 2012; Ma et al., 2016). Palaeoecological research indicates that both climatic

* Corresponding author.
E-mail address: zhaos@qfnu.edu.cn (S. Zhao).

https://doi.org/10.1016/j.aeolia.2018.09.004
Received 1 March 2018; Received in revised form 21 September 2018; Accepted 21 September 2018
Available online 01 October 2018
1875-9637/ © 2018 Elsevier B.V. All rights reserved.

change and human activities are responsible for shaping regional vegetation in the West Liao River Basin (Makohonienko et al., 2004; Li et al., 2006; Tarasov et al., 2006). Many researchers discussed man-environment relationships in the West Liao River Basin, and they concluded that environmental change had a significant effect on ancient civilizations, specifically on agricultural development (Deng, 1997; Xia et al., 2000; Hu et al., 2002; Jia et al., 2016a,b). This area occupies the marginal zone of millet agriculture due to both humidity (Jia et al., 2016a) and temperature (Jia et al., 2016b), which are probably the major constraints on the evolution of agriculture. However, which climatic factor (temperature or precipitation) is more important for agricultural development in the West Liao River Basin has not been tested by local palaeoclimatic records.

In the present paper we present a high-resolution palaeomoisture record spanning 4300–1000 cal. yr BP derived from multiple proxies of aeolian sediments of the Liuhutun section on the northeastern frontier of the Horqin sandy land, and assess the relative importance of temperature and precipitation in regional agricultural development by comparing palaeomoisture record with regional temperature changes and previous archeological studies from the West Liao River Basin.

2. Regional setting

The Horqin sandy land (42°40′–45°15′ N, 118°30′–124°30′ E; Fig. 1) covers an area of about 50,000 km^2 in northeast China, and is situated in the pastoral agricultural land. The region is characterized by a temperate continental monsoon climate, with the mean annual temperature varying from 3 to 7 °C (Wu, 2009). The mean annual precipitation ranges from ca. 500 mm in the southeast to ca. 350 mm in the northwest, with about 70% of the rainfall occurring in summer. The climate of this region is primarily influenced by the East Asian monsoon. The East Asian monsoon is caused by the land-sea thermal contrast between the Asian continent and the Pacific Ocean. In summer, East Asian summer monsoon (EASM) blows from the West Pacific and brings rainfall to the Horqin sandy land. In winter, the region is controlled by the Mongolia-Siberia high pressure zone, and northwesterly winds prevail. The mean annual wind speed is 3.5–4.5 m/s. Stabilized and partially stabilized dunes are widespread in the region. The zonal vegetation is woodland steppe (steppes with some small isolated oak forests). The zonal soil is kastanozem, which is in the process of being converted to aeolian sandy soils due to severe aeolian activity. Geomorphologically, the Horqin sandy land is situated in the Songliao plain which originated from the development of the Songliao subsidence zone. Quaternary sediments, comprising thick alluvial, lacustrine and aeolian deposits, are widespread in this region. These unconsolidated Quaternary deposits are composed of medium sand, fine sand, silt and clay, and provide plentiful source materials for the subsequent formation of sandy lands (Wu, 2009). Heavy mineral composition of modern sands support the supposition that they constitute reworked sediments initially deposited during the LGM (Xie and Ding, 2007).

3. Materials and methods

3.1. Lithology and sampling

The Liuhutun section (44° 28′ N, 123° 08′ E; 151 m a.s.l.) is located on a sandy sheet at the northeastern margin of the Horqin sandy land (Fig. 1). Landforms around the section are flat, gently undulating. The 2.96 m thick profile consists mainly of grayish yellow, medium to poor sorted, loose to slight compacted, non-stratified aeolian sands. A weak palaeosol, characterized by grey to taupe brown color and slight compact texture, was recognized at 2.30–2.64 m. Taupe brown palaeosols, characterized by compact to hard texture and occasional calcareous hyphae, were recognized at 0.18–0.88 m and 2.64–2.96 m. But, overall, the lithological changes are not significant (Fig. 2a). A total of 139 bulk samples were collected at 2 cm intervals (except for 0.84–1.20 m at 4 cm intervals). Seven radiocarbon samples were collected in order to provide a chronology. Samples were air-dried prior to measuring various physical and chemical parameters. All of the measurements below were made in the Key Laboratory of Western China's Environmental Systems (Ministry of Education), Lanzhou University.

3.2. Sediment dating methods

The conventional radiocarbon method was used for ^{14}C dating and the dated materials consisted of organic matter extracted from bulk samples after sieving the sediment to < 180 μm to remove any roots or macrofossils. The samples were pre-treated with acid and alkali (HCl

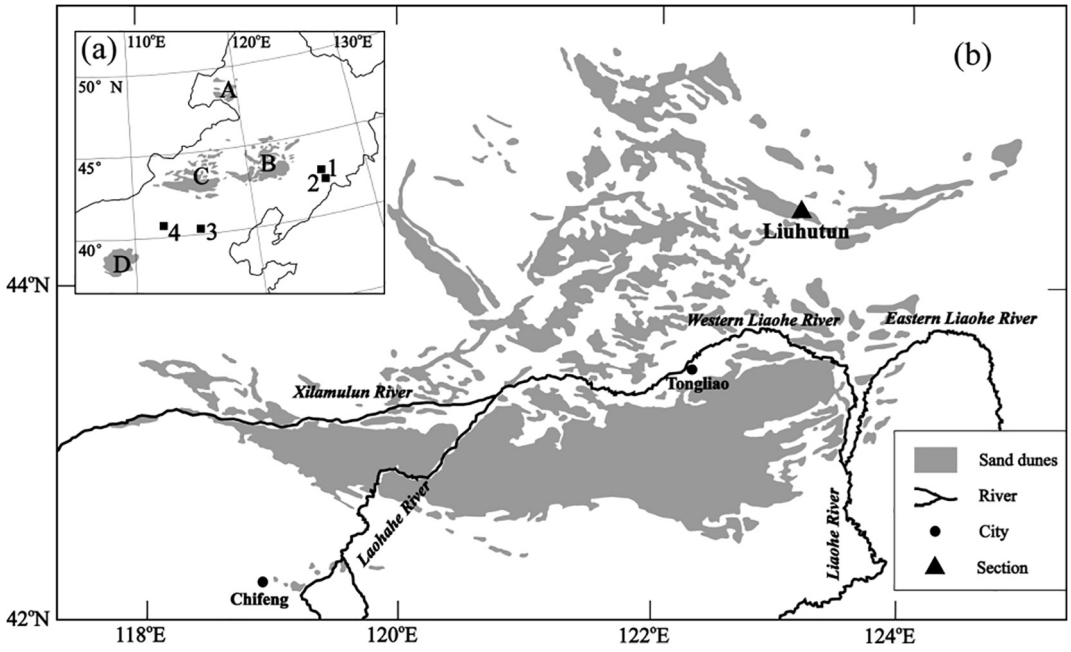

Fig. 1. Location of the Horqin sandy land and the Liuhutun section. Sandy lands are marked in figure (a) as follows: A, Hulun Buir; B, Horqin; C, Otindag; and D, Mu Us. Paleoclimatic records referred in this paper are marked with solid black squares in figure (a): 1, Hani; 2, Jinchuan; 3, Taishizhuang; and 4, Daihai.

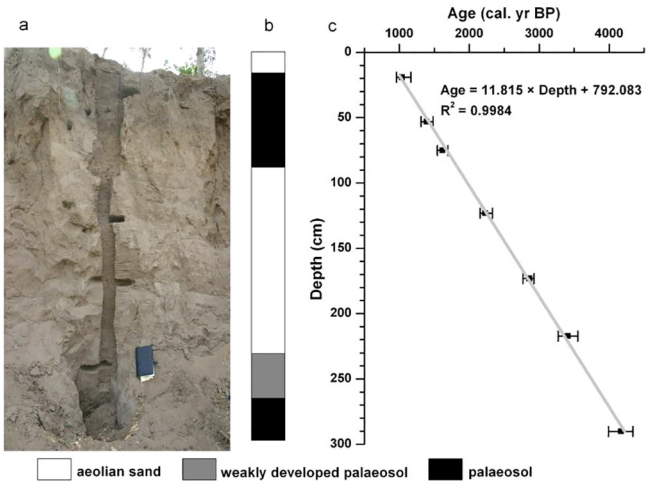

Fig. 2. Photograph (a), lithology (b) and age-depth model (c; squares and bars are ^{14}C dates with 1-σ errors) of the Liuhutun section.

2 M, NaOH 5%) and then dried, oxidized, and synthesized into benzene. The benzene was compounded for HIS-3 scintillation solutions, which were measured for about 1500 min after seven days.

3.3. Magnetic measurements

Magnetic parameters, especially magnetic susceptibility and magnetic grain-size, are widely used as moisture indicators in aeolian sediment studies, because of significant magnetic enhancement and ultrafine magnetic particle generation during pedogenesis (Liu et al., 2007).

The following series of magnetic measurements was made to characterize the magnetic mineral assemblages in the samples. Low frequency magnetic susceptibility (χ_{lf}) was measured using a Bartington Instruments MS2 meter. Anhysteretic remanent magnetization (ARM) was imparted using a LDA-3 AF demagnetizer with a peak AF field of 100 mT and a DC biasing field of 0.1 mT superimposed. The ARM is expressed as anhysteretic susceptibility (χ_{ARM}) by dividing by the biasing field strength. Saturation isothermal remanent magnetization (SIRM) was imparted in a 1 T field using a MMPM10 pulse magnetizer. All remanence measurements were made using a Molspin spinner magnetometer.

3.4. $CaCO_3$ measurements

The $CaCO_3$ content is an indicator of weathering intensity. In relatively arid areas, the $CaCO_3$ content is likely to be a sensitive indicator of precipitation and summer monsoon intensity due to the relatively weak leaching occurring during pedogenesis (Chen et al., 1997), during which the dissolved $CaCO_3$ tends to be reprecipitated in the top layer of the soil rather than being removed from the profile (Zhao, 1993). According to this pattern, there will be more $CaCO_3$ reprecipitated in the sediment when climate is humid (Zhao, 1993).

The $CaCO_3$ concentration was measured using the gas volumetric method. By adding excessive HCl to the samples, $CaCO_3$ was dissolved and generated CO_2. The $CaCO_3$ content was determined by measuring the volume of CO_2.

3.5. Organic matter content measurements

The organic matter content of aeolian deposits is usually regarded as an index of vegetation coverage and phytomass (Zhou et al., 1996; Xiao et al., 2002). In the desert-loess transitional zone of China, the type and degree of vegetation cover are controlled mainly by the summer monsoonal precipitation, and hence it can be used as an index of summer monsoon strength (Zhou et al., 1996; Xiao et al., 2002). When the summer monsoon circulation increased, the vegetation cover became denser, soil formation was initiated and thus the soil organic matter content increased.

The organic matter content was measured using the potassium dichromate-sulfating titrimetric method. With excessive H_2SO_4, $K_2Cr_2O_7$ oxidized organic carbon, and the Cr^{6+} was titrated with $FeSO_4$. The organic matter content was determined by the titration.

3.6. Grain-size measurements

In the study of aeolian deposits on the Chinese Loess Plateau (CLP), various grain-size parameters (e.g. median grain-size) have been widely used as a proxy index for the strength of the winter monsoon (Xiao et al., 1995, 2002). In addition, the sand (> 63 μm) content of aeolian deposits in the loess-desert transitional zone can be used as a proxy for the distance between the source and the accumulation zone, and hence the movement of the desert margin (Ding et al., 1999). The Liuhutun section lies in the northeastern margin of the Horqin sandy land, and therefore we infer that the grain-size distribution may reflect a combination of changes in wind strength and stages in the advance and retreat of the desert. Due to the sorting effect of wind, when the winter monsoon intensified, wind speed increased and grain-size became coarser; and when the desert shrank, the section became more distant from the source region and grain-size tended to be finer under the same wind strength. Both wind intensity and desertification are closely related with aeolian activity. Aeolian activity tends to be strong when wind intensity increased and desert expanded (Xiao et al., 1995; Ding et al., 1999).

The grain-size was measured using a Malvern Mastersizer 2000 laser grain-size analyzer, after being pretreated with H_2O_2 to remove organic matter, with HCl to remove carbonate and with $(NaPO_3)_6$ and ultrasonication to aid dispersal before measurement.

Table 1
Radiocarbon dating results of the Liuhutun section.

Depth (cm)	Dating material	^{14}C age (yr BP)	Calibrated age (cal. yr BP)		
			1-σ error range	2-σ error range	Median
19	Organic matter	1122 ± 58	958–1171	933–1176	1038
53	Organic matter	1495 ± 60	1311–1513	1302–1522	1391
75	Organic matter	1703 ± 60	1549–1696	1418–1808	1615
123	Organic matter	2224 ± 68	2153–2326	2056–2352	2226
173	Organic matter	2748 ± 75	2768–2924	2745–3056	2858
217	Organic matter	3180 ± 83	3256–3549	3181–3587	3402
290	Organic matter	3783 ± 89	3990–4294	3924–4418	4169

4. Results

4.1. Chronology

Seven radiocarbon dates (Table 1) were converted to calendar age (cal. yr BP) using the IntCal13 calibration curve implemented with the program CALIB 7.0.2 (Reimer et al., 2013). The calibrated dates are in good agreement with the stratigraphic sequence and there are no inversions (Fig. 2c). The age-depth model of the Liuhutun section was established by fitting a linear regression to the dates. As shown in Fig. 2c, this model is consistent with all of the measured ages within 1σ-calibrated age range. The Liuhutun section was deposited from about 4300 to 1000 cal. yr BP. The average sediment accumulation rate is 0.084 cm/yr with a theoretical time resolution of ca. 24 or 48 yr/sample. The chronological results indicate that the section has undergone roughly constant sediment accumulation, which may reflect a relatively stable wind regime during the interval of sediment accumulation. Stratigraphic chronology of the Liuhutun section shows that palaeosols were developed during 4300–3900 cal. yr BP and 1800–1000 cal. yr BP, that weak palaeosol was developed during 3900–3500 cal. yr BP, and that aeolian sand deposited during 3500–1800 cal. yr BP.

4.2. Magnetic grain-size

Magnetic grain-size parameters (e.g. χ_{ARM}/χ_{lf} and χ_{ARM}/SIRM) have been used in many studies of loess and aeolian sand deposits as indicators of pedogenic intensity and palaeoclimate, and especially palaeoprecipitation, which is the major factor influencing pedogenic intensity changes in an aeolian section (e.g. Nie et al., 2014; Chen et al., 2016; Zhao et al., 2016). In the Liuhutun section, we found that χ_{ARM}/χ_{lf} and χ_{ARM}/SIRM are more effective indicators of pedogenesis than is the magnetic susceptibility, as their changes are consistent with lithology (Fig. 3). However, in contrast to many other magnetic studies, they are inversely correlated to pedogenic intensity. As shown in Fig. 3, χ_{ARM}/χ_{lf} and χ_{ARM}/SIRM values are high in the aeolian sand layer (5.30 and 0.732 × 10^{-3} m/A in average, respectively), median in the weakly developed palaeosol layer (5.13 and 0.696 × 10^{-3} m/A in average, respectively), and low in the palaeosol layers (5.05 and 0.687 × 10^{-3} m/A in average, respectively). This may be because the detrital magnetic minerals from the source region were already very fine grained, i.e., stable single domain (SSD) (Zhao et al., 2013). Magnetic studies of the Liuhutun section indicate that the magnetic minerals consist of magnetite with a significant quantity of hematite and that magnetic grain-size is relatively fine, consisting mainly of SSD (of both aeolian and pedogenic origin) and superparamagnetic (SP, of pedogenic origin) grains, with a relatively narrow grain-size range (Zhao et al., 2013). Under natural conditions, fine-grained magnetite, which is generally more readily oxidized than coarse grained magnetite, oxidized to metastable maghemite or further oxidized to stable hematite. Therefore we infer that, during pedogenesis, on the one hand detrital SD (single domain) magnetite may be transformed into SP maghemite, and on the other hand that SD/SP maghemite may be further oxidized into hematite. χ_{ARM} is only sensitive to the content of SD ferrimagnetic minerals (magnetite and maghemite) (Peters and Dekkers, 2003), and the aforementioned mineral transitions occurring during pedogenesis will lead to the reduction of χ_{ARM}, and consequently to the observed inverse relationship between pedogenic intensity and χ_{ARM}/χ_{lf} and χ_{ARM}/SIRM.

The χ_{ARM}/χ_{lf} values range from 4.58 to 5.58, with an average value of 5.18, and the χ_{ARM}/SIRM values range from 0.617 × 10^{-3} m/A to 0.790 × 10^{-3} m/A, with an average value of 0.710 × 10^{-3} m/A. The two parameters present similar changes with time (depth). As shown in Fig. 3, χ_{ARM}/χ_{lf} and χ_{ARM}/SIRM are lowest at the basal palaeosol layer and gradually increasing during 4300–3800 cal. yr BP (2.96–2.54 m; range 4.58–5.22 and 0.617–0.719 × 10^{-3} m/A, 4.88 and 0.653 × 10^{-3} m/A in average, respectively), frequently fluctuating but overall at a high level during 3800–1700 cal. yr BP (2.54–0.76 m; range 5.02–5.58 and 0.683–0.790 × 10^{-3} m/A, 5.26 and 0.727 × 10^{-3} m/A in average, respectively), and overall low during 1700–1000 cal. yr BP (0.76–0.18 m; range 4.81–5.47 and 0.664–0.744 × 10^{-3} m/A, 5.16 and 0.706 × 10^{-3} m/A in average, respectively) with two peak periods around 1600–1400 cal. yr BP (0.68–0.52 m) and 1200–1000 cal. yr BP (0.34–0.18 m).

4.3. $CaCO_3$ content

The $CaCO_3$ content varies between 0.58% and 4.96%, with an

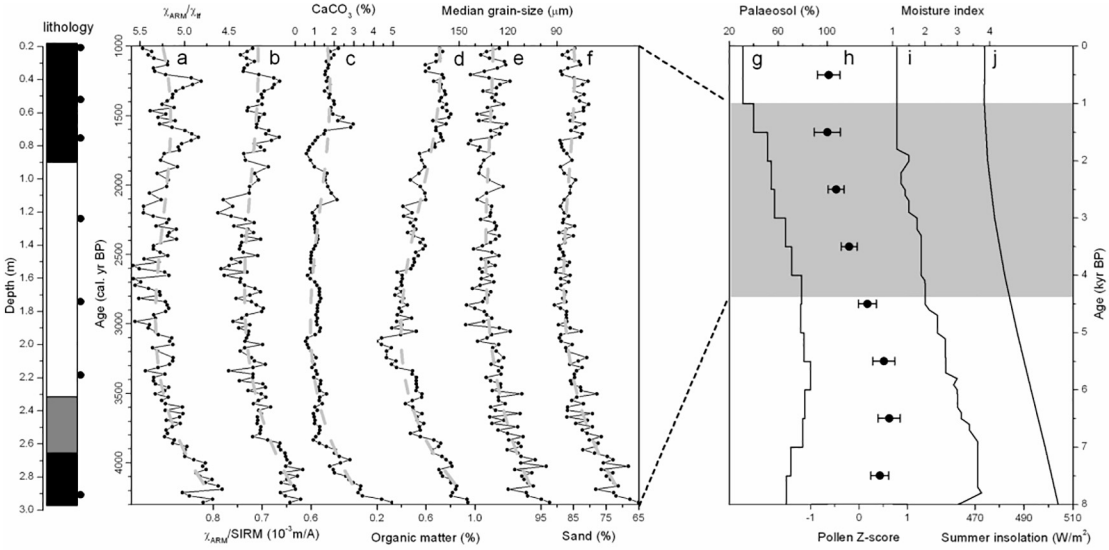

Fig. 3. Comparison of palaeoclimatic proxies of the Liuhutun section (a–f; dash lines indicate long-term trends) with various synthesized records of the East Asian summer monsoon and solar insolation. (g) synthesized sedimentary facies record for the East Sandy Lands (Hobq, Mu Us, Otindag, Horqin and Hulun Buir) of China (Li et al., 2014); (h) synthesized pollen index for the East Asian monsoon-margin region of China (Zhao and Yu, 2012); (i) pollen-based synthesized moisture index of eastern Inner Mongolia (Zhao et al., 2009b); and (j) Northern Hemisphere solar insolation changes in July at 30 °N (Berger and Loutre, 1991). Black dots beside the lithology indicate ^{14}C dating points.

average content of 1.48%. It is notable that the pedogenic layers tend to have a higher $CaCO_3$ content than do the sand layers (Fig. 3). The average $CaCO_3$ content for palaeosol layers (0.18–0.88 m and 2.64–2.96 m) is 2.05%, while, weakly developed palaeosol and aeolian sand layers (0.88–2.64 m) only have an average $CaCO_3$ content of 1.10%. As shown in Fig. 3, the $CaCO_3$ content achieves its highest value (4.96%) at the basal of the Liuhutun section (4300 cal. yr BP, 2.96 m), and then gradually decreases to 0.93% during 4300–3800 cal. yr BP (2.96–2.54 m). During 3800–1700 cal. yr BP (2.54–0.76 m), the $CaCO_3$ content is generally low, and the average value is only 1.07%. During 1700–1000 cal. yr BP (0.76–0.18 m), the $CaCO_3$ content is medium, and the average value is 1.82%.

4.4. Organic matter content

The organic matter content varies between 0.198% and 0.943%, with an average content of 0.572%. The organic matter content of palaeosol layers (range 0.548–0.943%, 0.731% in average) is obviously higher than that of weakly developed palaeosol and aeolian sand layers (range 0.198–0.721%, 0.471% in average). As shown in Fig. 3, the organic matter content achieves its highest value (0.943%) at the basal of the Liuhutun section (4300 cal. yr BP, 2.96 m), and then gradually deceases to 0.474% during 4300–3800 cal. yr BP (2.96–2.54 m). During 3800–1700 cal. yr BP (2.54–0.76 m), the organic matter content is generally low, in which the lowest value (0.198%) occurs at 3123 cal. yr BP (1.98 m), and the average value is only 0.488%. During 1700–1000 cal. yr BP (0.76–0.18 m), the organic matter content is high and steady (range 0.595–0.802%), and the average value is 0.714%.

4.5. Sediment grain-size

Grain-size frequency distribution curves for the Liuhutun section (Fig. 4) exhibit a characteristic bimodality, with the coarse component, which comprises most volume of the samples, possessing a modal size of 100–200 μm. This indicates that the samples consist mainly of a saltation component transported close to the ground surface by surface wind (Sun et al., 2002). The fine component (< 20 μm) consists of particles transported through long-distance suspension according to atmospheric dynamics researches (Sun et al., 2002). The relatively uniform grain-size frequency curves (Fig. 4) support the conclusion that the section represents a relatively stable depositional environment.

The Liuhutun section mainly consists of sand (> 63 μm), which comprises 65.06–90.83%, 83.99% in average, volume of the sediments. The median grain-size for the Liuhutun section ranges from 94.49 μm to 145.86 μm, with an average value of 126.83 μm. As shown in Fig. 3, these two parameters vary with time (depth) synchronously. The grain-size is finest (sand content 65.06%, median grain-size 94.49 μm) at the basal of the Liuhutun section (4300 cal. yr BP, 2.96 m), and then gradually coarsens during 4300–3000 cal. yr BP (2.96–1.90 m). During 3000–1700 cal. yr BP (1.90–0.76 m), the grain-size is overall coarse, and the average values for the sand content and median grain-size are 87.78% and 133.39 μm, respectively. During 1700–1000 cal. yr BP (0.76–0.18 m), grain-size is slightly finer than during 3800–1700 cal. yr BP (2.54–0.76 m), and average values for the sand content and median grain-size are 84.5% and 130.41 μm, respectively.

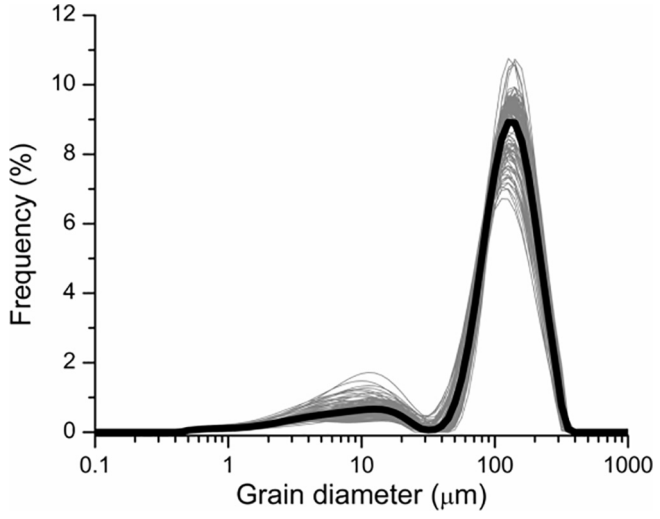

Fig. 4. Grain-size frequency distribution curves of samples from the Liuhutun section. The bold black line is the average curve.

5. Discussion

5.1. Climate change recorded by Liuhutun section

All of the environmental proxies measured for the Liuhutun section (Fig. 3a–f) exhibit a very similar long-term trend over time. The records of organic matter, $CaCO_3$ content and magnetic grain-size parameters (χ_{ARM}/χ_{lf} and χ_{ARM}/SIRM) of the Liuhutun section indicate that in the Horqin sandy land, moisture condition from 4300 to 1000 cal. yr BP exhibits three distinctive periods with 3800 cal. yr BP and 1700 cal. yr BP as boundaries: (i) 4300–3800 cal. yr BP, characterized by high but gradually decreasing organic matter and $CaCO_3$ content, and low but gradually increasing χ_{ARM}/χ_{lf} and χ_{ARM}/SIRM, was the wettest period with a drying trend; (ii) 3800–1700 cal. yr BP, characterized by low organic matter and $CaCO_3$ content, and high χ_{ARM}/χ_{lf} and χ_{ARM}/SIRM, was generally dry; (iii) and 1700–1000 cal. yr BP, characterized by moderate organic matter content, $CaCO_3$ content, χ_{ARM}/χ_{lf} and χ_{ARM}/SIRM, was sub-humid. The grain-size of the Liuhutun section indicate that aeolian activity was relatively weak during 4300–3000 cal. yr BP with a gradual trend of strengthening, and is relatively strong between 3000 and 1000 cal. yr BP with a slightly weak interval during 1700–1000 cal. yr BP.

5.2. Comparison with other records

The long-term climatic trend recorded by the Liuhutun section roughly parallels synthesized percentage frequency of palaeosol dates for the sandy lands (Hobq, Mu Us, Otindag, Horqin and Hulun Buir) of northern China (Li et al., 2014; Fig. 3g) and pollen-based synthesized moisture index for the eastern Inner Mongolia (Zhao et al., 2009b; Fig. 3i). Furthermore, pollen-based synthesized moisture indices from the summer monsoon-influenced semi-arid belt (Wang and Feng, 2013), a synthesis of pollen indices from the East Asian monsoon-margin region (Zhao and Yu, 2012; Fig. 3h), and the general trend of relative aridity changes inferred from a synthesis of palaeoenvironmental records in the Badain Jaran Desert and other dryland regions in China (Yang et al., 2011), all suggest a moisture maximum during the mid-Holocene, and a dry late Holocene with a gradual trend of increasing aridity. All of the findings referred above (Zhao et al., 2009b; Yang et al., 2011; Zhao and Yu, 2012; Wang and Feng, 2013; Li et al., 2014) are consistent with the moisture record of the Liuhutun section, which in turn track the North Hemisphere summer insolation (Berger and Loutre, 1991; Fig. 3j). It seems that climate change within the vast East Asian monsoon zone is controlled by the same system, and that late Holocene climate change within the Horqin sandy land was a direct response to the variation of the strength of the East Asian monsoon circulation. Many previous researches suggest that during the Holocene the East Asian summer monsoon progressively weakened and retreated southeastwards as the Northern Hemisphere summer insolation declined as a result of earth orbital forcing (An et al., 2000; Jiang and Liu, 2007; Zhao et al., 2016). This supposed relationship between insolation and monsoon circulation is confirmed by numerical modeling experiments (Jiang et al., 2013). The coherence between climate change in the Horqin sandy land and Northern Hemisphere summer insolation

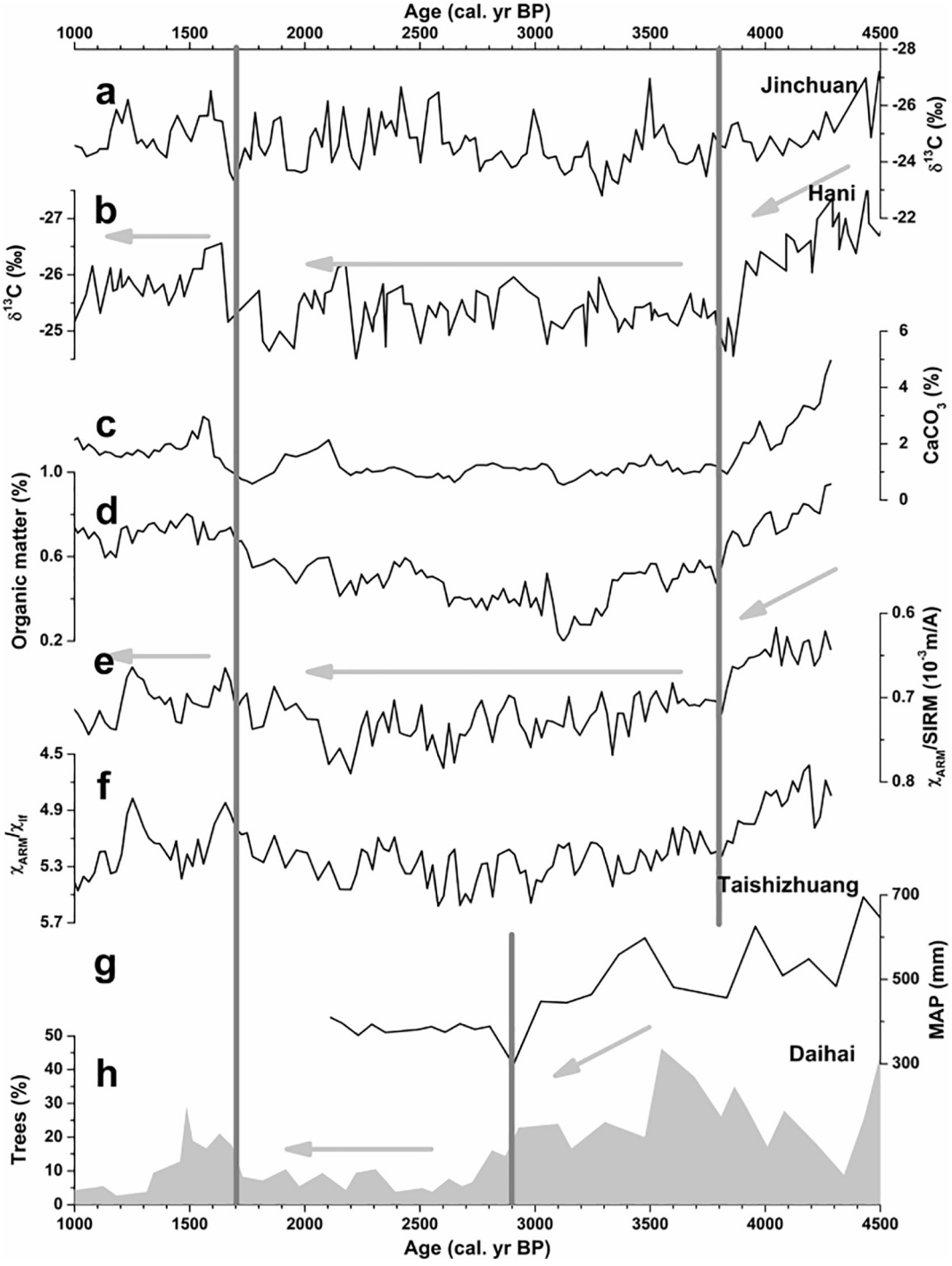

Fig. 5. Late Holocene moisture evolution in Horqin sandy land and the nearby areas. $\delta^{13}C$ of peat cellulose for the Jinchuan (a; Hong et al., 2001) and Hani (b; Hong et al., 2005) cores; moisture proxies for the Liuhutun section (c–f); pollen-based mean annual precipitation reconstructed from the Taishizhuang site (g; Tarasov et al., 2006); and pollen record from the Daihai Lake (h; Xiao et al., 2004).

suggests that, at least during the late Holocene, the long-term trend of climate change in the study area was driven by orbitally-induced change in solar insolation. The decrease of summer insolation during the late Holocene may reduce the land-sea thermal contrast between the Asian continent and the Pacific Ocean and weaken the East Asian monsoon (Zhao et al., 2016).

Comparisons with moisture records from the surrounding areas demonstrate that summer monsoon variations recorded by $\delta^{13}C$ of peat cellulose in Jinchuan (Hong et al., 2001; Fig. 5a) and Hani (Hong et al., 2005; Fig. 5b), northeastern China, exhibit three stages with a very similar timing to those at Liuhutun. Pollen records from the Taishizhuang site (Tarasov et al., 2006; Fig. 5g), and a sediment core from Daihai Lake (Xiao et al., 2004; Fig. 5h), about four degrees of latitude south of the Liuhutun section, exhibit similar characteristics to the records from northeastern China, except that the mid-Holocene humid climate at Taishizhuang and Daihai continued until 2900 cal. yr BP, and thus it lagged behind northeastern China. This may be attributed to the gradual retreat of the East Asian summer monsoon (An et al., 2000; Jiang and Liu, 2007). In addition, Taishizhuang and Daihai experienced an abrupt drought corresponding to the 4.2 kyr event (Bond et al.,

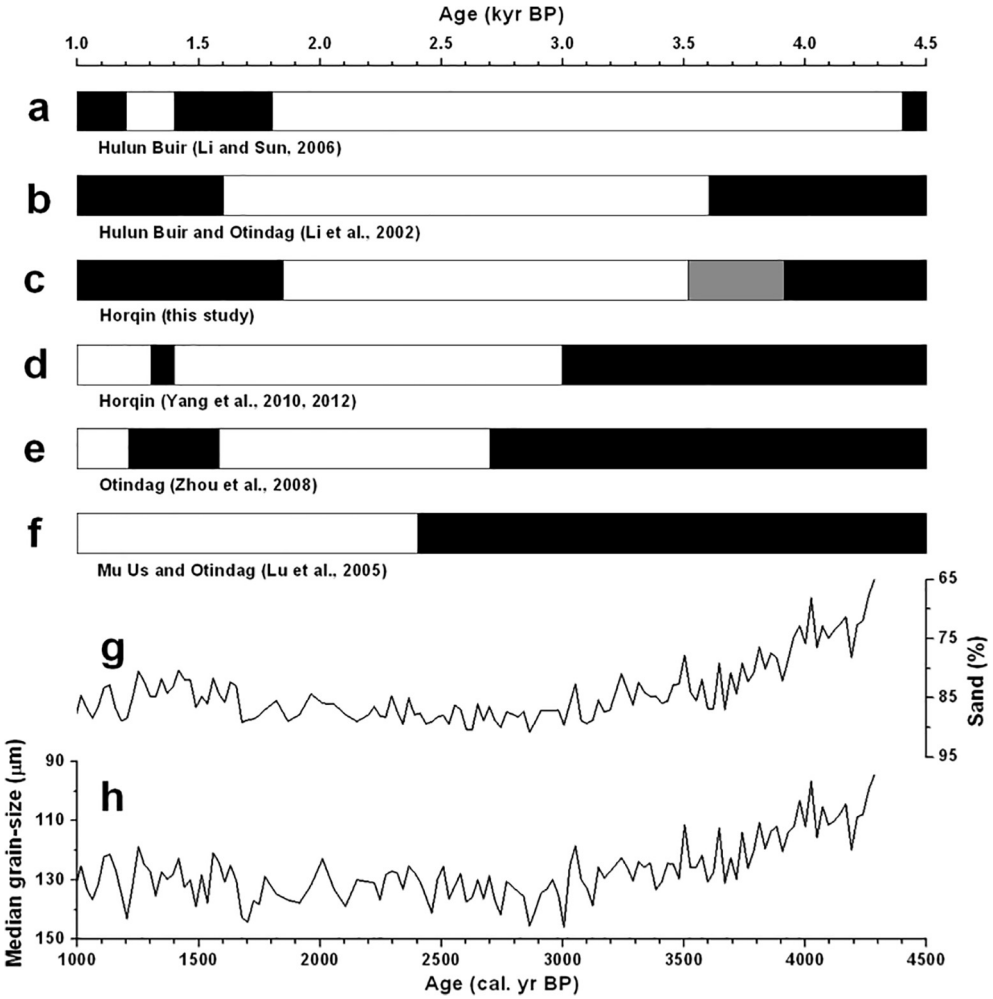

Fig. 6. Dune stabilization and sandy soil development inferred from the OSL-dated stratigraphic records of the sandy lands in northern China (a–f) and grain-size of Liuhutun section (g, h).

1997), while Jinchuan, Hani and Liuhutun experienced gradually increasing aridity. This phenomenon was probably the result of a decrease in evaporation induced by a fall in temperature which in higher latitudes tends to compensate for the abrupt reduction in precipitation (An et al., 2006).

Stratigraphic chronology and grain-size records of the Liuhutun section are consistent with the results of previous optically stimulated luminescence (OSL) dating of aeolian sand in the Horqin sandy land which indicate that there was a phase of considerable dune stabilization during 8–3 kyr, and multiple episodes of stabilization and mobilization after 3 kyr (Yang et al., 2010, 2012; Fig. 6d). In recent years, the results of many OSL chronology studies of sandy lands in northern China, e.g. Hulun Buir, Horqin, Otindag and Mu Us, suggest a humid climate and dune stabilization during the mid-Holocene and that the dunes began to mobilize gradually in the late Holocene (Li et al., 2002; Lu et al., 2005; Li and Sun, 2006; Zhou et al., 2008; Yang et al., 2010, 2012; Fig. 6a–f). The timing of the mobilization of the dunes changed gradually on a latitudinal gradient, becoming later from north to south and thereby confirming the gradual weakening and retreat of the East Asian summer monsoon (An et al., 2000; Jiang and Liu, 2007).

5.3. Climate change and prehistory agricultural development

In the Horqin sandy land (West Liao River Basin), there has been a series of ancient civilizations since the Holocene, including Xiaohexi culture, Xinglongwa culture, Zhaobaogou culture, Hongshan culture, Xiaoheyan culture, Lower Xiajiadian culture and Upper Xiajiadian culture (Yang, 1994; Shelach, 1999; Linduff et al., 2002–2004). Archaeobotanical researches demonstrate that this region is one of the origin centers of dryland agriculture in north China (Zhao, 2011; Liu et al., 2012; Ma et al, 2016), that people began to domesticate millet during the Xiaohexi period (before 8500 cal. yr BP) (Ma et al, 2016), and that human adoption of millet as a staple crop happened between 7800 and 7300 cal. yr BP (Liu et al., 2012). Archaeological remains demonstrate that the Lower Xiajiadian period (ca. 4000–3400 cal. yr BP) is the heyday of prehistoric agriculture (Hu et al., 2002; Wang, 2004, 2007; Shelach et al., 2011; Wagner et al., 2013). Subsistence was based on millet farming supplemented with animal husbandry and hunting during the Lower Xiajiadian period (Shelach, 1999; Hu et al., 2002; Wang, 2004, 2007; Jia et al., 2016a). After the Lower Xiajiadian period, animal husbandry began to prevail, the proportion of agriculture shrank and the number of archaeological site decreased (Wang, 2004; Shelach et al., 2011; Wagner et al., 2013; Jia et al., 2016a).

Historical and palaeo-environmental researches demonstrate that climate conditions, specifically temperature and precipitation, have an important impact on agricultural development (Hinsch, 1988; Su et al., 2014; Fang et al., 2015). Climatic proxies from the Liuhutun section show that the agriculture prevailing period (ca. 4000–3400 cal. yr BP; Shelach, 1999; Hu et al., 2002; Wang, 2004, 2007; Jia et al., 2016a) is relatively humid, especially at the early stage (Fig. 7), which may have provided plenty of water for the development of dryland agriculture. However, both this study and other palaeoprecipitation records (Hong

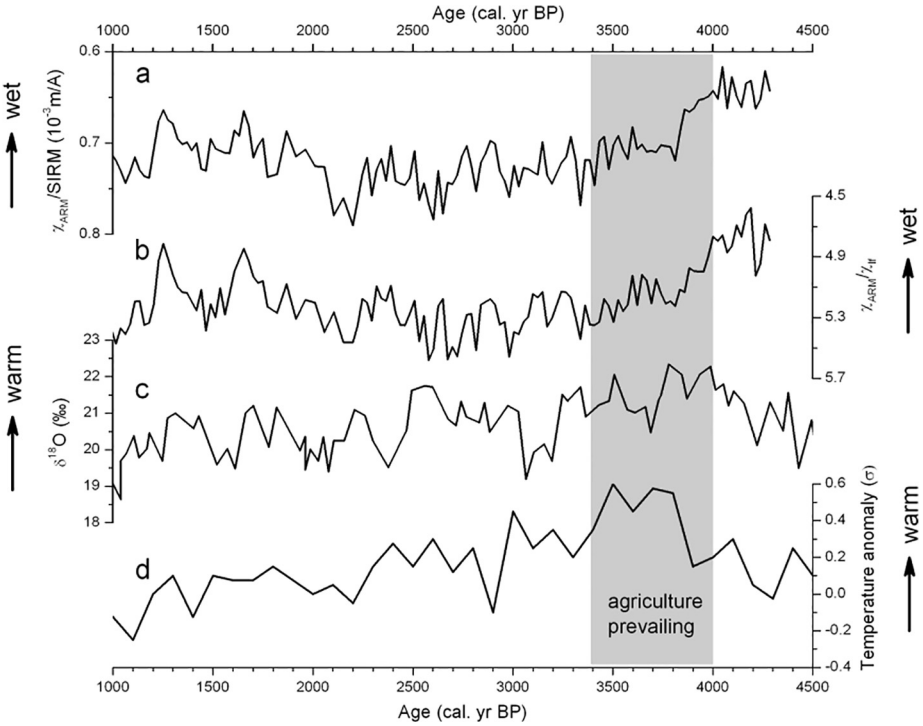

Fig. 7. Comparison of moisture proxies of Liuhutun section (a, b) with $\delta^{18}O$ of peat cellulose for the Hani peat core (c; Hong et al., 2009) and synthesized temperature reconstruction sequences of China (d; Ge et al., 2006). Gray shadow indicate the agriculture prevailing period (ca. 4000–3400 cal. yr BP) inferred from published archeology data (Shelach, 1999; Hu et al., 2002; Wang, 2004, 2007; Jia et al., 2016a).

et al., 2001, 2005; Xiao et al., 2004; Tarasov et al., 2006) indicate that there have more precipitation during 4300–4000 cal. yr BP (Late Xiaoheyan period), but agriculture at that time was less developed compared with the Lower Xiajiadian period, and subsistence was mainly based on hunting and gathering (Deng, 1997; Xia et al., 2000; Hu et al., 2002). We thus infer that precipitation may not have been a limiting factor for agricultural development in this region. In contrast, a peat cellulose $\delta^{18}O$ record from Hani peat mire (Hong et al., 2009; Fig. 7c), northeastern China, and a synthesized temperature reconstruction sequence of China (Ge et al., 2006; Fig. 7d) indicate that temperature during the Lower Xiajiadian period is the highest in the late Holocene. Pollen and oxygen isotope analyses of the Taishizhuang peat section also indicate that significant cold events occurred during the Xiaoheyan period (ca. 5000–4000 cal. yr BP) and that significant warming occurred during the Lower Xiajiadian period (Jin and Liu, 2004). Therefore we propose the hypothesis that temperature may have played a more important role in regional agriculture than precipitation.

Broomcorn millet (*Panicum miliaceum*) and foxtail millet (*Setaria italica*) are important dryland crops in northern China. Archaeobotanical researches demonstrate that millets are major crops of the Lower Xiajiadian Culture within the West Liao River Basin (Zhao et al., 2009a; Jia et al., 2016a). The drought-tolerant and thermophilic phenological properties of millets (d'Alpoim Guedes, 2013) may enable agriculture flourished during the warmest rather than the wettest period. Historical documents of China also indicate that agricultural output is positively correlated with temperature (Su et al., 2014; Fang et al., 2015), while only moderate precipitation generate bumper grain production, and more or less precipitation beyond the optimal range could result in floods and droughts, both of which tend to reduce agricultural yields (Su et al., 2014). High temperature and moderate precipitation may have facilitated millet's cultivation during the Lower Xiajiadian period.

6. Conclusions

The novelty of this work lies in that we have reconstructed the late Holocene palaeomoisture variations of the Horqin sandy land from multi-proxy analyses of aeolian deposit, and investigated the relative importance of temperature and precipitation in regional agriculture development by comparing moisture records with regional temperature and subsistence strategy changes. Results show that 4300–3800 cal. yr BP was a humid period with a drying trend; 3800–1700 cal. yr BP was generally dry; and 1700–1000 cal. yr BP was sub-humid. The Liuhutun record is consistent with other palaeoclimatic records for the region and surrounding areas as well as with the entire East Asian monsoon zone. It is clear that the regional climate was responsive to monsoonal circulation driven by variations in Northern Hemisphere summer insolation. High temperature and moderate precipitation may have facilitated agricultural development during the Lower Xiajiadian period (ca. 4000–3400 cal. yr BP). As a result of the drought-tolerant and thermophilic attributes of millets, temperature may have had a more important effect on regional agriculture than precipitation.

7. CRediT author statement

Shuang Zhao: Conceptualization, Methodology, Data Curation, Writing - Original Draft. Dunsheng xia: Conceptualization, Writing - Review & Editing, Supervision. Heling Jin: Validation, Resources, Supervision. Jia Jia: Methodology, Investigation, Data Curation. **Bing Liu:** Investigation, Visualization.

Acknowledgements

This work was financially supported by the Open Foundation of MOE Key Laboratory of Western China's Environmental System, Lanzhou University and the Fundamental Research Funds for the Central Universities (lzujbky-2018-kb01) and the National Natural Science Foundation of China (Grants 41671204 and 41877444).

Appendix A. Supplementary data

Supplementary data to this article can be found online at https://doi.org/10.1016/j.aeolia.2018.09.004.

References

An, C.-B., Feng, Z.-D., Barton, L., 2006. Dry or humid? Mid-Holocene humidity changes in arid and semi-arid China. Quat. Sci. Rev. 25 (3–4), 351–361.

An, Z., Porter, S.C., Kutzbach, J.E., Wu, X., Wang, S., Liu, X., Li, X., Zhou, W., 2000. Asynchronous Holocene optimum of the East Asian monsoon. Quat. Sci. Rev. 19 (8), 743–762.

Berger, A., Loutre, M.F., 1991. Insolation values for the climate of the last 10 million years. Quat. Sci. Rev. 10 (4), 297–317.

Bond, G., Showers, W., Cheseby, M., Lotti, R., Almasi, P., deMenocal, P., Priore, P., Cullen, H., Hajdas, I., Bonani, G., 1997. A pervasive millennial-scale cycle in North Atlantic Holocene and glacial climates. Science 278 (7), 1257–1266.

Chen, F., Jia, J., Chen, J., Li, G., Zhang, X., Xie, H., Xia, D., Huang, W., An, C., 2016. A persistent Holocene wetting trend in arid central Asia, with wettest conditions in the late Holocene, revealed by multi-proxy analyses of loess-paleosol sequences in Xinjiang, China. Quat. Sci. Rev. 146, 134–146.

Chen, F.H., Bloemendal, J., Wang, J.M., Li, J.J., Oldfield, F., 1997. High-resolution multi-proxy climate records from Chinese loess: evidence for rapid climatic changes over the last 75 kyr. Palaeogeogr. Palaeoclimatol. Palaeoecol. 130 (1–4), 323–335.

d'Alpoim Guedes, J., 2013. Adaptation and Invention during the Spread of Agriculture to Southwest China. Harvard University, Cambridge.

deMenocal, P.B., 2001. Cultural responses to climate change during the late Holocene. Science 292, 667–673.

Deng, H., 1997. The change of the man-land relationship in the northern Yanshan Mountain region during megathermal. Acta Geog. Sin. 52 (1), 63–71 (in Chinese).

Ding, Z., Sun, J., Rutter, N.W., Rokosh, D., Liu, T., 1999. Changes in sand content of loess deposits along a north-south transect of the Chinese Loess Plateau and the implications for desert variations. Quat. Res. 52 (1), 56–62.

Fang, X.Q., Su, Y., Yin, J., Teng, J.C., 2015. Transmission of climate change impacts from temperature change to grain harvests, famines and peasant uprisings in the historical china. Sci. China Earth Sci. 58 (8), 1427–1439.

Ge, Q., Wang, S., Zheng, J., 2006. Reconstruction of temperature series in China for the last 5000 years. Prog. Nat. Sci. 16 (8), 838–845.

Hinsch, B., 1988. Climatic change and history in China. J. Asian Hist. 22 (2), 131–159.

Hong, Y.T., Hong, B., Lin, Q.H., Shibata, Y., Hirota, M., Zhu, Y.X., Leng, X.T., Wang, Y., Wang, H., Yi, L., 2005. Inverse phase oscillations between the East Asian and Indian Ocean summer monsoons during the last 12 000 years and paleo-El Niño. Earth Planet. Sci. Lett. 231 (3–4), 337–346.

Hong, Y.T., Hong, B., Lin, Q.H., Shibata, Y., Zhu, Y.X., Leng, X.T., Wang, Y., 2009. Synchronous climate anomalies in the western North Pacific and North Atlantic regions during the last 14,000 years. Quat. Sci. Rev. 28 (9), 840–849.

Hong, Y.T., Wang, Z.G., Jiang, H.B., Lin, Q.H., Hong, B., Zhu, Y.X., Wang, Y., Xu, L.S., Leng, X.T., Li, H.D., 2001. A 6000-year record of changes in drought and precipitation in northeastern China based on a $\delta^{13}C$ time series from peat cellulose. Earth Planet. Sci. Lett. 185 (1), 111–119.

Hu, J., Cui, H., Li, Y., 2002. Reconstruction of the evolution history of man-land system since the Holocene in the Xiliaohe River Basin. Sci. Geog. Sin. 22 (5), 535–542 (in Chinese).

Jia, X., Lee, H.F., Zhang, W., Wang, L., Sun, Y., Zhao, Z., Yi, S., Huang, W., Lu, H., 2016a. Human-environment interactions within the West Liao River Basin in Northeastern China during the Holocene Optimum. Quat. Int. 426, 10–17.

Jia, X., Sun, Y., Wang, L., Sun, W., Zhao, Z., Lee, H.F., Huang, W., Wu, S., Lu, H., 2016b. The transition of human subsistence strategies in relation to climate change during the Bronze Age in the West Liao River Basin, Northeast China. Holocene 26 (5), 781–789.

Jiang, D., Lang, X., Tian, Z., Ju, L., 2013. Mid-Holocene East Asian summer monsoon strengthening: insights from Paleoclimate Modeling Intercomparison Project (PMIP) simulations. Palaeogeogr. Palaeoclimatol. Palaeoecol. 369 (1), 422–429.

Jiang, W.Y., Liu, T.S., 2007. Timing and spatial distribution of mid-Holocene drying over northern China: response to a southeastward retreat of the East Asian Monsoon. J. Geophys. Res. 112, D24111. https://doi.org/10.1029/2007JD009050.

Jin, G., Liu, D., 2004. Mid-Holocene climate change in North China, and the effect on cultural development. Chin. Sci. Bull. 47 (5), 408–413.

Li, Q., Wu, H., Yu, Y., Sun, A., Marković, S.B., Guo, Z., 2014. Reconstructed moisture evolution of the deserts in northern China since the Last Glacial Maximum and its implications for the East Asian Summer Monsoon. Global Planet. Change 121 (10), 101–112.

Li, S.-H., Sun, J., 2006. Optical dating of Holocene dune sands from the Hulun Buir Desert, northeastern China. Holocene 16 (3), 457–462.

Li, S.-H., Sun, J.-M., Zhao, H., 2002. Optical dating of dune sands in the northeastern deserts of China. Palaeogeogr. Palaeoclimatol. Palaeoecol. 181 (4), 419–429.

Li, Y.Y., Willis, K.J., Zhou, L.P., Cui, H.T., 2006. The impact of ancient civilization on the northeastern Chinese landscape: palaeoecological evidence from the Western Liaohe River Basin, Inner Mongolia. Holocene 16 (8), 1109–1121.

Linduff, K.M., Drennan, R.D., Shelach, G., 2002–2004.. Early complex societies in NE China: the Chifeng international collaborative archaeological research project. J. Field Archaeol. 29 (1/2), 45–73.

Liu, B., Jin, H., Sun, Z., 2011. Climate change in east Horqin sandy land since 6.0 ka BP. J. Desert Res. 31 (6), 1398–1405 (in Chinese).

Liu, Q., Deng, C., Torrent, J., Zhu, R., 2007. Review of recent developments in mineral magnetism of the Chinese loess. Quat. Sci. Rev. 26 (3–4), 368–385.

Liu, X., Jones, M.K., Zhao, Z., Liu, G., O'Connell, T.C., 2012. The earliest evidence of millet as a staple crop: new light on Neolithic foodways in North China. Am. J. Phys. Anthropol. 149 (2), 283–290.

Lu, H., Miao, X., Zhou, Y., Mason, J., Swinehart, J., Zhang, J., Zhou, L., Yi, S., 2005. Late Quaternary aeolian activity in the Mu Us and Otindag dune fields (north China) and lagged response to insolation forcing. Geophys. Res. Lett. 32, L21716. https://doi.org/10.1029/2005GL024560.

Ma, Z.K., Yang, X.Y., Zhang, C., Sun, Y.G., Jia, X., 2016. Early millet use in West Liaohe area during early-middle Holocene. Sci. China Earth Sci. 59 (8), 1554–1561.

Makohonienko, M., Kitagawa, H., Naruse, T., Nasu, H., Momohara, A., Okuno, M., Fujiki, T., Liu, X., Yasuda, Y., Yin, H., 2004. Late-Holocene natural and anthropogenic vegetation changes in the Dongbei Pingyuan (Manchurian Plain), northeastern China. Quat. Int. 123–125, 71–88.

Mu, Y., Qin, X., Zhang, L., Xu, B., 2016. Holocene climate change evidence from high-resolution loess/paleosol records and the linkage to fire-climate change-human activities in the Horqin dunefield in northern China. J. Asian Earth Sci. 121, 1–8.

Nie, J., Stevens, T., Song, Y., King, J.W., Zhang, R., Ji, S., Gong, L., Cares, D., 2014. Pacific freshening drives Pliocene cooling and Asian monsoon intensification. Sci. Rep. 4, 5474. https://doi.org/10.1038/srep05474.

Peters, C., Dekkers, M.J., 2003. Selected room temperature magnetic parameters as a function of mineralogy, concentration and grain size. Phys. Chem. Earth. 28 (16–19), 659–667.

Reimer, P.J., Bard, E., Bayliss, A., Beck, J.W., Blackwell, P.G., Ramsey, C.B., Buck, C.E., Cheng, H., Edwards, R.L., Friedrich, M., Grootes, P.M., Guilderson, T.P., Haflidason, H., Hajdas, I., Hatté, C., Heaton, T.J., Hoffmann, D.L., Hogg, A.G., Hughen, K.A., Kaiser, K.F., Kromer, B., Manning, S.W., Niu, M., Reimer, R.W., Richards, D.A., Scott, E.M., Southon, J.R., Staff, R.A., Turney, C.S.M., van der Plicht, J., 2013. IntCal13 and marine13 radiocarbon age calibration curves 0–50,000 years cal BP. Radiocarbon 55 (4), 1869–1887.

Shelach, G., 1999. Leadership Strategies, Economic Activity, and Interregional Interaction: Social Complexity in Northeast China. Kluwer Academic/Plenum Publishers, New York.

Shelach, G., Raphael, K., Jaffe, Y., 2011. Sanzuodian: the structure, function and social significance of the earliest stone fortified sites in China. Antiquity 85 (327), 11–26.

Su, Y., Fang, X.Q., Yin, J., 2014. Impact of climate change on fluctuations of grain harvests in china from the western Han Dynasty to the Five Dynasties (206 BC–960 AD). Sci. China Earth Sci. 57 (7), 1701–1712.

Sun, D., Bloemendal, J., Rea, D.K., Vandenberghe, J., Jiang, F., An, Z., Su, R., 2002. Grain-size distribution function of polymodal sediments in hydraulic and aeolian environments, and numerical partitioning of the sedimentary components. Sed. Geol. 152 (3–4), 263–277.

Tarasov, P., Jin, G., Wagner, M., 2006. Mid-Holocene environmental and human dynamics in northeastern China reconstructed from pollen and archaeological data. Palaeogeogr. Palaeoclimatol. Palaeoecol. 241 (2), 284–300.

Wagner, M., Tarasov, P., Hosner, D., Fleck, A., Ehrich, R., Chen, X., Leipe, C., 2013. Mapping of the spatial and temporal distribution of archaeological sites of northern China during the Neolithic and Bronze Age. Quat. Int. 290–291 (2), 344–357.

Wang, L., 2004. The evolution of cultural pattern and economic formation in the western Liaoning area from the Xia to the Warring States period. Acta Archaeol. Sin. 3, 243–270 (in Chinese).

Wang, L., 2007. The economic pattern and environmental context of lower Xiajiadian culture reflected by the excavation data of Dashanqian site. Res. China's Front. Archaeol. 6 (1), 350–357 (in Chinese).

Wang, W., Feng, Z., 2013. Holocene moisture evolution across the Mongolian Plateau and its surrounding areas: a synthesis of climatic records. Earth-Sci. Rev. 122 (3), 38–57.

Wang, X., Chen, F., Zhang, J., Yang, Y., Li, J., Hasi, E., Zhang, C., Xia, D., 2010. Climate, desertification, and the rise and collapse of China's historical dynasties. Hum. Ecol. 38 (1), 157–172.

Wu, Z., 2009. Sandy Deserts and its Control in CHINA. Science Press, Beijing.

Xia, Z., Deng, H., Wu, H., 2000. Geomorphologic background of the prehistoric cultural evolution in the Xar Moron River Basin, Inner Mongolia. Acta Geogr. Sin. 55 (3), 329–336 (in Chinese).

Xiao, J., Nakamura, T., Lu, H., Zhang, G., 2002. Holocene climate changes over the desert/loess transition of north-central China. Earth Planet. Sci. Lett. 197 (1–2), 11–18.

Xiao, J., Porter, S.C., An, Z., Kumai, H., Yoshikawa, S., 1995. Grain size of quartz as an indicator of winter monsoon strength on the Loess Plateau of central China during the last 130,000 Yr. Quat. Res. 43 (1), 22–29.

Xiao, J., Xu, Q., Nakamura, T., Yang, X., Liang, W., Inouchi, Y., 2004. Holocene vegetation variation in the Daihai Lake region of north-central China: a direct indication of the Asian monsoon climatic history. Quat. Sci. Rev. 23 (14), 1669–1679.

Xie, J., Ding, Z.L., 2007. Compositions of heavy minerals in Northeastern China sand lands and provenance analysis. Sci. China Ser. D 50 (11), 1715–1723.

Yang, H., 1994. The archaeological sequence and stages for overlapping Neolithic and Bronze Age cultures in Liaoxi region. Cultural Relics 5, 37–52 (in Chinese).

Yang, L.H., Wang, T., Zhou, J., Lai, Z.P., Long, H., 2012. OSL chronology and possible forcing mechanisms of dune evolution in the Horqin dunefield in northern China since the Last Glacial Maximum. Quat. Res. 78 (2), 185–196.

Yang, L.H., Zhou, J., Lai, Z.P., Long, H., Zhang, J.R., 2010. Lateglacial and Holocene dune evolution in the Horqin dunefield of northeastern China based on luminescence dating. Palaeogeogr. Palaeoclimatol. Palaeoecol. 296 (1), 44–51.

Yang, X., Scuderi, L., Paillou, P., Liu, Z., Li, H., Ren, X., 2011. Quaternary environmental changes in the drylands of China — A critical review. Quat. Sci. Rev. 30 (23), 3219–3233.

Yi, S., Lu, H., Xu, L., Zeng, Z., 2013. Paleoclimate changes and reconstruction of the border of Horqin dunefield (northeastern China) since the Last Glacial Maximum. Quat. Sci. 33 (2), 206–217 (in Chinese).

Zhao, H., Lu, Y., Yin, J., 2007. Optical dating of Holocene sand dune activities in the Horqin sand-fields in inner Mongolia, China, using the SAR protocol. Quat. Geochronol. 2 (1–4), 29–33.

Zhao, J., 1993. CaCO3 and sedimentary environment of loess strata. Acta Sedimentol. Sin.

11 (1), 136–142 (in Chinese).
Zhao, K., Li, X., Shang, X., Zhou, X., Sun, N., 2009a. Agricultural characteristics of middle-late Bronze Age in western Liaoning province. Chin. Bull. Bot. 44 (6), 718–724 (in Chinese).
Zhao, S., Xia, D., Jin, H., Li, G., 2013. Magnetic characteristics of aeolian sand sediments in Horqin sandy land, northeastern China, and its paleoenvironmental significance: a preliminary exploration. J. Desert Res. 33 (2), 334–342 (in Chinese).
Zhao, S., Xia, D., Jin, H., Jia, J., Li, G., Gao, F., Wang, Y., 2016. Long-term weakening of the East Asian summer and winter monsoons during the mid- to late Holocene recorded by aeolian deposits at the eastern edge of the Mu Us Desert. Palaeogeogr. Palaeoclimatol. Palaeoecol. 457, 258–268.
Zhao, Y., Yu, Z., 2012. Vegetation response to Holocene climate change in East Asian monsoon-margin region. Earth-Sci. Rev. 113 (1–2), 1–10.
Zhao, Y., Yu, Z., Chen, F., 2009b. Spatial and temporal patterns of Holocene vegetation and climate changes in arid and semi-arid China. Quat. Int. 194 (1), 6–18.
Zhao, Z., 2011. New archaeobotanic data for the study of the origins of agriculture in China. Curr. Anthropol. 52 (S4), S295–S306.
Zhou, W., Donahue, D.J., Porter, S.C., Jull, T.A., Li, X., Stuiver, M., An, Z., Matsumoto, E., Dong, G., 1996. Variability of monsoon climate in East Asia at the end of the last glaciation. Quat. Res. 46 (3), 219–229.
Zhou, Y.L., Lu, H.Y., Mason, J., Miao, X.D., James, S., Ronald, G., 2008. Optically stimulated luminescence dating of aeolian sand in the Otindag dune field and Holocene climate change. Sci. China Ser. D 51 (6), 837–847.